 https://doi.org/10.24191/jeesr.v20i1.006

Deep Learning Approach for Blur Detection of Digital Breast Tomosynthesis Images

Nur Athiqah Harron*, Siti Noraini Sulaiman, Muhammad Khusairi Osman, Iza Sazanita Isa, Noor Khairiah A. Karim and Mohd Ikmal Fitri Maruzuki

Abstract—**Image quality is critical in domains such as computer vision, image processing, and pattern recognition. One of the areas of image processing where image quality is critical is image restoration. In the field of medical imaging, blur detection is used in the pre-processing stage of medical image restoration. It was noted that blurring has the potential to obscure small cancers and microcalcifications. As a result, some abnormalities were undiscovered until they have grown significantly. The quality of an image can be determined whether it is blurry using various blur detection algorithms. This paper presents a comparative study of various pre-trained convolutional neural networks (CNNs) models as feature extraction for blur detection. The CNNs models are ResNet18, ResNet50, AlexNet, VGG16 and InceptionV3. These CNNs were then connected to a classifier known as support vector machine (SVM) to classify DBT images into blurry or not blurry. To evaluate the performance of the pre-trained CNN as features extractor, statistical performance measures namely the accuracy, receiver-operating characteristics (ROC), area under the curve (AUC), and execution time were employed. According to the evaluation results, InceptionV3 has the best accuracy rate at 0.9961 with AUC of 0.9961. Most of the output of Pre-trained CNN with SVM lies closest to the ideal ROC curve near the top left corner. AlexNet has the shortest processing time of any of the CNNs model. The findings of this study might be used as reference before performing image restoration.**

Index Terms—Blur detection, features extraction, convolutional neural network, Digital breast tomosynthesis

This manuscript is submitted on 13th January 2022 and accepted on 28th June 2022. The research is funded by the Ministry of Higher Education Grant Scheme (FRGS) No: FRGS/1/2021/TK0/UITM/02/19, the Research Management Centre (RMC), Universiti Teknologi MARA (UiTM), College of Engineering UiTM Cawangan Pulau Pinang, Kampus Permatang Pauh, Malaysia, and Advanced Medical & Dental Institute Universiti Sains Malaysia (AMDI, USM) for all support given in this study.

N. A. Harron[1], S. N. Sulaiman[1,2], M. K. Osman[1], I. S. Isa[1] and M. I. F. Maruzuki[1] are [1]Centre for Electrical Engineering Studies, Universiti Teknologi MARA, Cawangan Pulau Pinang, Permatang Pauh, 13500 Pulau Pinang, MALAYSIA and [2]Integrative Pharmacogenomics Institute (iPROMISE), UiTM Puncak Alam Campus, Bandar Puncak Alam, Puncak Alam, Selangor, 42300, Malaysia (e-mail: nurathiqah742@uitm.edu.my, sitinoraini@uitm.edu.my,khusairi@uitm.edu.my, izasazanita@uitm.edu.my and ikmalf@uitm.edu.my).

N. K. A. Karim is with Advanced Medical and Dental Institute, Universiti Sains Malaysia Bertam, Kepala Batas Penang, Malaysia. (e-mail: drkhairiah@usm.my).

*Corresponding author
Email address: nurathiqah742@uitm.edu.my

I. INTRODUCTION

AUTOMATIC quality analysis of medical images has emerged as a significant area of research. However, automatic blur detection in DBT images has received insufficient research. Breast tomosynthesis is a technique that extends digital mammography by acquiring a sequence of projection images at various angles of the x-ray source concerning the breast. To provide a three-dimensional picture of the breast while maintaining as much full-field digital mammography (FFDM) acquisition geometry as possible, the DBT technique was created [1]–[3]. The DBT is a cone-beam, restricted-angle (15–60°) tomographic approach that allows for the reconstruction of the entire breast volume from a series of projection-view mammograms. Reconstruction artefacts are likely to occur due to the lower acquisition angle. Several research have been conducted on both human subjects and phantoms to evaluate and enhance the DBT image quality [4]–[6]. In addition, acquisition time could contribute to motion artefact and consequently less distinct depiction of calcification. As the acquisition time of tomosynthesis is longer, there may be motion artefacts that could result in obscuring small calcifications [7].

Blurring is a known DBT phenomenon that arises during image acquisition. It has been reported to reduce lesion detection performance and mask small microcalcifications, leading to failure in detecting smaller abnormalities at early stage until they reach more advanced stages, particularly in dense breast tissue [8]. Early detection of breast cancer is the key to provide higher survival rates for breast cancer patients. Therefore, the accuracy of proper diagnosis relies on sufficient radiologic image quality in order to obtain high-quality, artefact-free, and blur-free images [9]. One of the most difficult aspects of working with digital images captured in uncontrolled environments is determining whether or not the image is of sufficient quality to be further studied. In this case, blur is one of the most common causes of digital image quality reduction, particularly in images obtained with limited angular range and movable device like DBT. The limited angular sampling in DBT results in out-of-plane artefacts in the z-direction. The out-of-plane artefacts appear as a blurred version of in-plane objects in the direction of tube motion [10]. Due to this blurry artefacts issue, developing methods for analysing the blur distortion of DBT acquired images for diagnostic purposes is crucial.

There are two types of image quality assessment (IQA) measures: subjective and objective [11], [12]. Human observers are used in the first group of methods to assess image quality, whereas the latter determines an objective quality score. Subjective approaches, by their very nature, can become arduous, time-consuming, and costly; as a result, preference is given in searching for solutions, while the objective approaches are normally conducted without the intervention of humans as the objective systems capable of

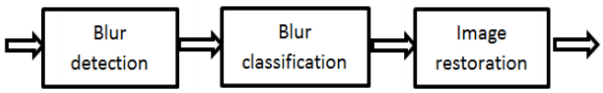

Fig. 1. Block diagram to relate blur detection, blur classification, and image restoration [14]

quickly analysing images and reporting their quality. Additionally, when doing visual quality assurance (QA), technologists usually examine images on low-resolution monitors like those typically used by remote operations panels (ROPs) in the exam room or other convenient areas. These monitors yield a low-resolution display for comparing blur in radiographs to the diagnostic-quality displays used by radiologists. As a result, minor to moderate blur may go unnoticed during the visual quality assurance process, resulting in images with little diagnostic value in their image archiving and communication systems (PACS) that influence image diagnosis [13].

Image quality is critical in computer vision, image processing, and other related domains. Image restoration is a subcategory of image processing in which the quality of the input image is critical. Blur detection is a stage in the image restoration process known as pre-processing. By utilising various blur detection algorithms, the quality of an image may be determined whether it is blurry or not. Then, image restoration can be applied to the blurry image.

The study of [14] categorises the public domain research on blur images into three primary phases as shown in Fig. 1. However, this paper concentrates only on the stage of image blur detection that considers the blur or sharp estimation. The long-term goal of the research is to keep a comparable number of extracted feature points while using a sharp image and to increase the number of correctly matched feature points when using an input blur image. Blur detection techniques are advantageous for image blur detection since they are utilised as a preliminary step in identifying images that require image restoration or deblurring.

II. BLUR DETECTION METHODS

Blur detection is a vital and intriguing subject in computer vision. A critical aspect of blur detection is the process of identifying effective features to distinguish between distorted and undistorted image parts. Numerous techniques exist for resolving this issue, most of them utilise the two-step procedure to discern between clear and blurred regions. The first phase entails manually creating separated components in an image based on a set of empirical data in gradient format. After that, a binary classifier is used to differentiate the warped and clear regions. The Laplacian variance and CNN are two essential approaches for detecting blurred images, and they are the subject of this review.

A. Laplacian Variance

This method is implemented to discover edges in a picture. It is additionally a derivative operator but the basic contrast between different operators like Sobel, Kirsch and Laplacian operator is that all other derivatives are first-order derivative masks. The Laplacian operator is further separated into two classifications which are the positive Laplacian operator and negative Laplacian operator [15].

Laplacian attempts to de-emphasize portions in an image by gradually varying grey levels and emphasising grey level discontinuities [16]. This derivative operator produces images with grey edge lines and some discontinuities on a black background. Thus, an image's exterior and interior edges are created [17]. There are numerous methods for determining the blurriness of an image, but the best and simplest is to use the variance of the Laplacian technique, which returns a single floating-point value representing the image's "blurriness"[17]. This approach does nothing more than convolving input image with the Laplacian operator and computing the variance. If the variance is less than a predetermined value, the image is considered blurry. A high variance as stated in [18] is a normal representative in-focus image indicating the presence of a large number of responses for both non-edge like and edge like. Similarly, a low detected variance indicates that there is little response dispersion, implying that the image has few edges. Thus, it can be concluded that if an image has a small number of edges, it is blur.

Therefore, choosing an appropriate threshold value is entirely dependent on the domain. If the threshold is set incorrectly, images will be labelled as blurry. For example, if an image is not blurry and the threshold is set incorrectly, the image will be recorded as blurry and vice versa. In this paper Laplacian operator is used to assess the degree of blurriness so that it can construct a class for blur or not-blur in the blur detection process. There is currently no radiologist-developed standard for determining the degree of blur.

B. Convolutional Neural Networks (CNNs)

Convolutional neural networks (CNNs) are a subset of deep learning techniques that have garnered considerable attention for their capacity to solve picture classification issues and as a tool for extracting representation features from input images [19]. In certain cases, they have been used as components of systems that do more complex tasks. Girshick et al. (2013) [20] employed CNNs as feature extractors in object recognition and localization system. The study that utilised CNN in the field of medical imaging is extensively used today to continuously improve the workload of healthcare providers and integrate the use of the CAD system in clinical settings just as it is with natural image processing.

In the last five years, deep learning-based models have outperformed classical methods in a wide variety of computer vision tasks, including generic object detection and recognition[21], semantic segmentation[22], depth reconstruction[23], saliency detection[24], image captioning, denoising, super-resolution, and deconvolution[25]–[27], and facial expression recognition[28], [29]. It is widely known that the success of deep CNN models largely depends on their extraordinary capacity to generalise and extract useful features directly from input images for difficult classification problems [30].

In conjunction with the availability of big data storage and increased processing capabilities over the years, researchers have successfully developed pre-trained networks with a variety of layers and depths that have been trained on massive datasets such as ImageNet for public usage. [31]. When trained on large datasets of a variety of images, CNN is considered a powerful deep learning approach; it can learn rich feature representations for a wide range of images from these vast databases. These representations of features frequently outperform handcrafted features. Utilizing a pretrained CNN as a feature extractor is a simple approach to exploit the capability of CNNs without investing time and effort in training. Instead of using image features such as HOG or SURF, features are extracted using CNN. As blur

represents a deterioration of image quality, blur detection is distinct from most recognition issues, which allow for multiple degradation factors such as noise or blur. However, to detect blur, we must learn blur-related features while accepting the enormous variance introduced by varied image content.

Therefore, this paper examines various pretrained CNN as feature extractor on DBT images and use those features to train an image classifier for blur detection and compares their performance in terms of accuracy rate and execution time. The proposed method will be discussed in detail in the following section.

III. METHODS

This section describes the method to perform a comparative analysis of image blur detection using various pre-trained CNNs. Fig. 3 depicts a flowchart of the experimental procedure. This study was programmed and tested in MATLAB R2021a, using a notebook with AMD Ryzen 5 3500U CPU @ 2.10GHz processor and 8.0 GB RAM with the Windows 10, 64bit operating system.

A. Dataset

This study intends to assess the capability of deep learning approach to detect blur of 200 DBT images. To the best of our knowledge, there is no publicly available image quality dataset that includes DBT images in their search to deblur the quality of the images. In this study, the public DBT images dataset from [32] is used. The dataset consist of DBT RGB images with 1890x2457 pixels in size. The input image for network training is augmented to fit the network input size.

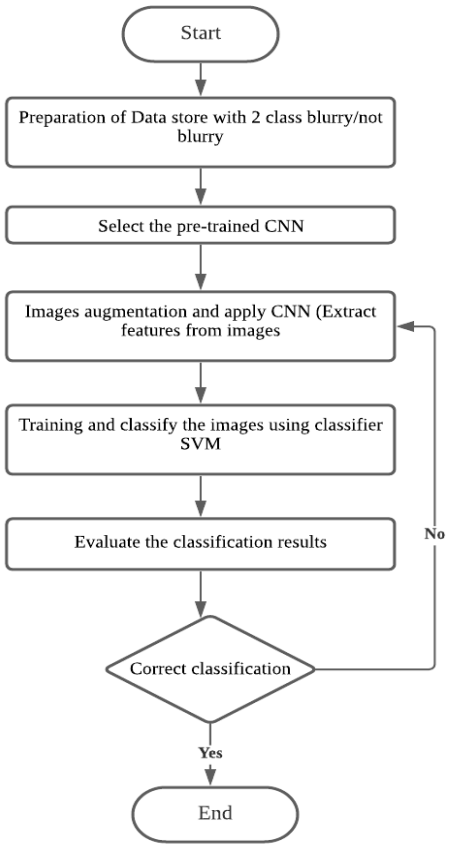

Fig. 3. Summarized flowchart of the experimental procedure

The Laplacian method is used to choose the image based on the variance value and threshold setting to construct a class for blur and not blurry images for the network datastore as in Fig. 2 illustrates the sample of images from blurry and not

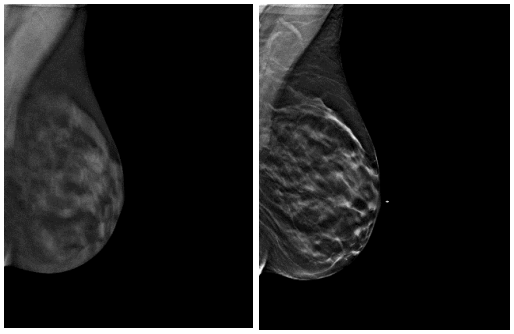

(a) Blurry (b) Not Blurry

Fig. 2. DBT image example for each class in dataset (a) blurry and (b) not blurry

blurry DBT image classes. An expert's knowledge was used to set the ground truth dataset where the experts are required to select the appropriate threshold. Based on the dataset, 70% of the images in each class were utilised as the training dataset, with the remainder 30% serving as the validation collection. In this code, the 'MiniBatchSize' is set at 32 for each experimental training to ensure that the CNN and image data fit into the CPU memory.

B. CNN Pre-trained Networks and feature extraction

In this study, AlexNet (8 layers), ResNet18(18 layers) and ResNet50 (50 layers), VGG16 (16 layers) and InceptionV3 (48 layers) are chosen as feature extractor. Alexnet (8 layers) architecture was proposed by Krizhevsky et al. in 2012 [31], where 227 x 227 pixels on RGB channels input images were needed for this model. It consists of eight layers; the first five layers are made of convolutional and maxpooling layers, while the last three are fully connected layers stacked on each other. It was trained using an extensive visual database known ImageNet using more than 14 million natural images, classified into 1000 image classes[31].

After the success of AlexNet, many other deeper architectures have been proposed such as ResNet. ResNet architecture demonstrated to be very effective on the ILSVRC 2015 (ImageNet Large Scale Visual Recognition Challenge) validation set with a top1-recognition accuracy of about 80% [33]. ResNet-18 with 18 layers deep and ResNet-50 with 50 layers deep architecture had an image input size of 224-by-224, which is about 10 times and 20 times deeper than AlexNet, respectively. On the other hand, VGGNet-16[34] is made up of 16 convolutional layers and is particularly appealing due to its uniform architecture. Like AlexNet, it contains only 3x3 convolutions but large number of filters. It is now the community's most favoured method for extracting features from images [35]. Finally, Inception v3 is a popular image recognition model that has been demonstrated to achieve higher than 78.1 percent accuracy on the ImageNet dataset. The model represents the result of several ideas explored over time by various researchers [36].

The models used in this paper are widely different. The VGG16-model can be considered as the traditional and parameter greedy model. InceptionV3-model is the widest model, while ResNet50-model is the deepest model. AlexNet-

model is the smallest model. A summary of all the information is tabulated in Table I. ResNet50 and InceptionV3 have the largest number of layers and biggest depth among the others. As the layer and the depth of the network increase, the training becomes slow, and the network architecture becomes large.

TABLE I.
PRETRAINED CNNS MODEL ARCHITECTURE

	AlexNet	ResNet 18	ResNet 50	VGG16	Inceptio nV3
Image Input Size	227x227 x3	224x224 x3	224x224 x3	224x224 x3	299x299 x3
Total Layers	25	71	177	41	315
Depth	8	18	50	16	48
Size	227MB	44MB	96MB	515MB	89MB
Parameters (M)	61.0	11.7	25.6	138	23.9

However, compared to VGG, the model size is smaller due to the use of global average pooling instead of fully connected layer in VGG. The larger number of parameters in VGG results in higher inference time.

Each layer of a CNN responds or activates to an input image. However, only a few layers of a CNN are sufficient for image feature extraction. The first layer of the network captures fundamental visual properties like edges and blobs. Deeper network layers then process these basic data, combining them to generate higher-level image features. These higher-level features are more suited for recognition tasks because they incorporate all the primitive features into a richer image representation [33].

In this experiment the weights initialization of the first convolution layer are shown in Fig. 4. The first layer of the network has learned filters for capturing blob and edge features. Then the image features are extracted from deeper layers using activation methods at the layer just before the fully connected networks. For the classifier, SVM is used to classify blurry or not blurry DBT images. In the testing stage, the test features extracted by the CNN, are then passed to the SVM classifier.

C. Blur Detection Using Support Vector Machine

A sophisticated classification algorithm, developed by Vapnik [37] is the support vector machine (SVM). It is based on the structural risk minimization principle, which seeks to minimise the bound on the generalisation error (i.e., the error generated by the learning machine on data not observed during training) rather than the mean square error over the training data set. As a result, when applied to data outside of the training set, an SVM tends to perform well.

A classifier that has been trained to recognise blur in radiographs is used to detect blur in images. Feature vectors produced from images in CNN activation layers are included in the training data. The classifier assesses the attributes of a test image and outputs a probability indicating the presence of blur in the image. The procedure is repeated to extract image features from testing dataset. The features obtained during the testing are then passed to the classifier to measure the accuracy of the trained classifier. The obtainable results are used for comparisons in terms of execution time, accuracy, ROC and AUC. The true positive (TP), true negative (TN), false positive (FP) and false negative (FN) values from obtainable confusion matrix are used to calculate the system performance accuracy as denoted Table II. By plotting TPR against FPR rates, ROC probability curve and AUC are evaluated.

TABLE II
METRICS FOR SYSTEM PERFORMANCE EVALUATION

Measure Performance	Equation
TPR	*TP/(TP+FN)*
FPR	*FP/(TN+FP)*
Accuracy	*(TP+TN)/(TP+FN+TN+FP)*

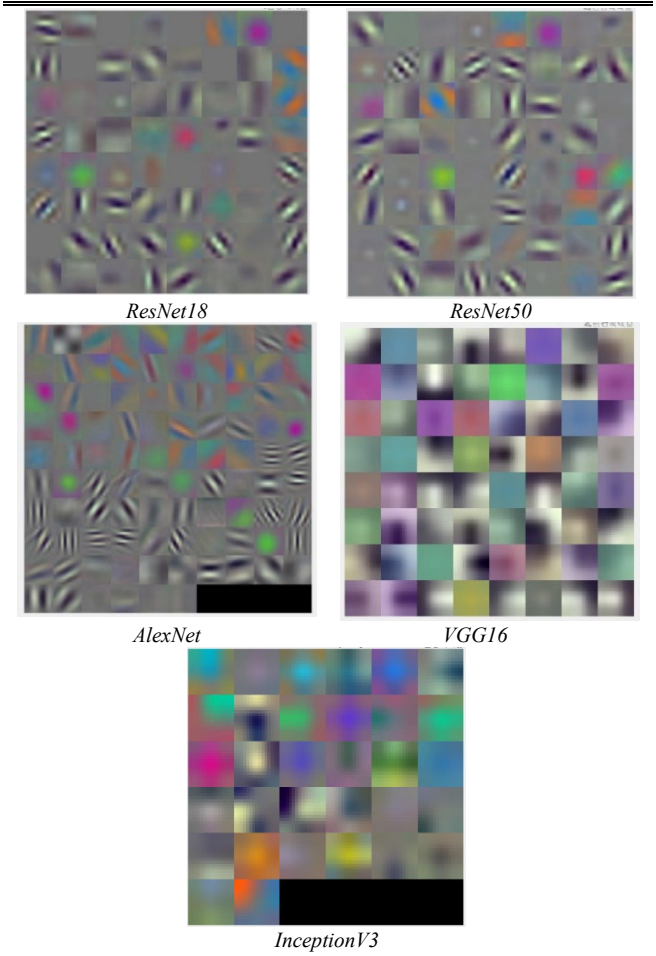

Fig. 4. First convolution layer weights for each of Pre-trained CNN of the executed experiment.

IV. RESULT AND DISCUSSIONS

The performance of the trained system is observed when different pretrained CNN as features extractor is applied on the same dataset. Meanwhile, the effect of CNN architecture is investigated and finally the performance of the trained classifier is evaluated. In this study, the performance was evaluated based on its ability to classify blurry or not blurry DBT images. Table III compares the results obtained from the experimental analyses of the blurry detection system.

To evaluate the performance of the algorithm, the ROC curve is used which provides a graphical representation of the trade-off between the false-negative and false-positive rates for every possible cut off. The obtained ROC curves are presented in Fig. 5 to compare the performance of three widely used pretrained CNN. Meanwhile, the measurement of each performance parameter is tabulated in Table III. It shows that the classifier using SVM with pre-trained CNN lies closest to the ideal ROC curve near the top left corner

with an AUC value greater than 95% for each of the CNNs. It is noticed that InceptionV3 and ResNet-50 outperform other architectures with largest AUC 0.9961 and 0.9947 as shown in Fig. 6, though the difference is not significant and can be attributed to randomness in the training process.

TABLE III
RESULT FROM THE EXPERIMENTAL ANALYSIS OF BLURRY DETECTION USING DIFFERENT PRE-TRAINED CNNS AND SVM.

	Pre-Trained CNN +SVM				
	ResNet-18 (18 layers)	**ResNet-50 (50 layers)**	**AlexNet (8 layers)**	**VGG16 (16layer)**	**InceptionV3 (48 layers)**
AUC	0.9858	0.9947	0.9839	0.9768	**0.9961**
Accuracy	0.9583	0.9750	0.9580	0.9420	**0.9670**
Execution Time	1min 35sec	3min 12sec	**0 min 40sec**	7min 51sec	4min 25sec

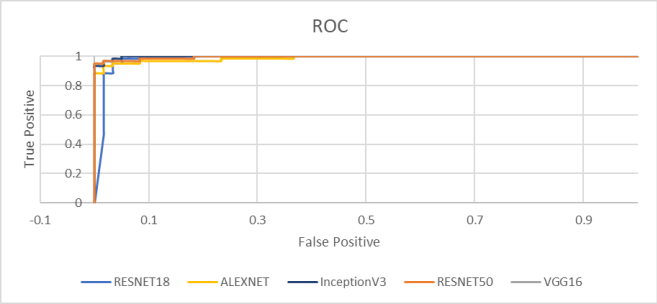

Fig. 5. ROC performance of pre-trained CNNs with SVM classifier

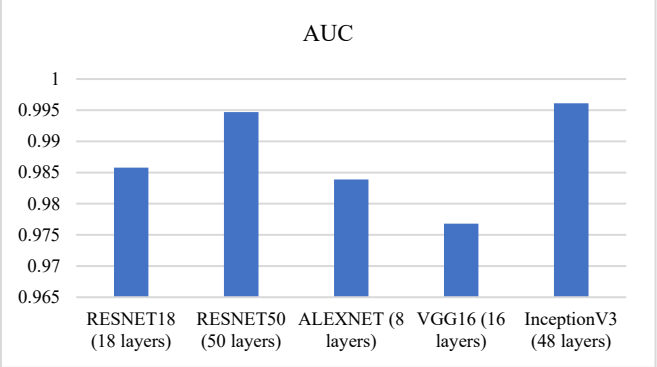

Fig. 6. AUC for different pre-trained CNNs

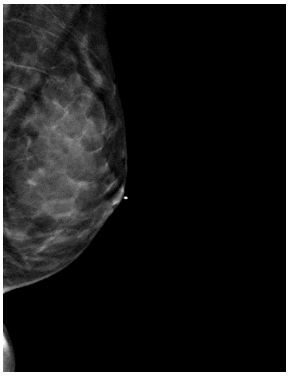

Fig. 7 Sample ambiguous DBT image considered as blurry by the expert and not blurry by the system.

The misclasify case analysis reveals that the diversity in normal DBT structures is significant when compared to the differences in lack of sharpness that would differentiate a diagnostically acceptable image from one that should be rejected. Another reason for failure is improper feature representation of the blur region, which occurs most frequently in a local region. As a result, the motion blur can no longer be detected. Fig 7. shows an ambiguous image sample considered as blurry by the expert and not blurry by the system.

V. CONCLUSIONS

In this investigation, the aim was to assess the performance of deep learning approach towards blur detection of DBT images. The application of the pre-trained CNN features with classifier SVM to the blur classification of DBT images has shown good results. InceptionV3 shows the best result in term of accuracy at 97% and largest AUC at 0.9961. In terms of execution time, AlexNet has the fastest processing time. As the next stage of this project, we plan to conduct a comparative analysis of the different image restoration or deblurring techniques that can be used to achieve our long-term goal.

ACKNOWLEDGMENT

This research work is financially supported by Ministry of Higher Education Grant Scheme (FRGS) (Ref: FRGS/1/2021/TK0/UITM/02/19. The authors would like to express their gratitude to members of the Advanced Control System and Computing Research Group (ACSCRG), Advanced Rehabilitation Engineering in Diagnostic and Monitoring Research Group (AREDiM), Integrative Pharmacogenomics Institute (iPROMISE), and Centre for Electrical Engineering Studies, Universiti Teknologi MARA, Cawangan Pulau Pinang for their assistance and guidance during the fieldwork. The authors are grateful to Universiti Teknologi MARA, Cawangan Pulau Pinang for their immense administrative and financial support. Special thanks to the Imaging Department, Advanced Medical and Dental Institute, Universiti Sains Malaysia, Kepala Batas, Pulau Pinang for the professional consultation and expert guide.

VI. REFERENCES

[1] L. E. Niklason *et al.*, 'Digital Tomosynthesis In Breast Imaging'', *Radiology*, vol. 205, pp. 399–406, 1997.

[2] T. Wu *et al.*, 'Tomographic mammography using a limited number of low-dose cone-beam projection images', *Med. Phys.*, vol. 30, no. 3, pp. 365–380, 2003, doi: 10.1118/1.1543934.

[3] T. Wu, R. H. Moore, E. A. Rafferty, and D. B. Kopans, 'A comparison of reconstruction algorithms for breast tomosynthesis', *Med. Phys.*, vol. 31, no. 9, pp. 2636–2647, 2004, doi: 10.1118/1.1786692.

[4] Z. Yiheng *et al.*, 'A comparative study of limited-angle cone-beam reconstruction methods for breast tomosynthesis', *Med Phys.*, vol. 33, no. 10, pp. 3781–3795, 2006, doi: 10.1118/1.223754.

[5] I. Andersson *et al.*, 'Breast tomosynthesis and digital mammography: A comparison of breast cancer visibility and BIRADS classification in a population of cancers with subtle mammographic findings', *Eur. Radiol.*, vol. 18, no. 12, pp. 2817–2825, 2008, doi: 10.1007/s00330-008-1076-9.

[6] T. Wu, R. H. Moore, and D. B. Kopans, 'Voting strategy for artifact reduction in digital breast tomosynthesis', *Med. Phys.*, vol. 33, no. 7, pp. 2461–2471, 2006, doi: 10.1118/1.2207127.

[7] M. L. Spangler *et al.*, 'Detection and classification of calcifications on digital breast tomosynthesis and 2D digital mammography: A comparison', *Am. J. Roentgenol.*, vol. 196, no. 2, pp. 320–324, 2011, doi: 10.2214/AJR.10.4656.

[8] P. Hogg, K. Szczepura, J. Kelly, and M. Taylor, 'Blurred digital mammography images', *Radiography*, vol. 18, no. 1, pp. 55–56, 2012, doi: 10.1016/j.radi.2011.11.008.

[9] N. Kamona and M. Loew, 'Automatic detection of simulated

motion blur in mammograms', *Med. Phys.*, vol. 47, no. 4, pp. 1786–1795, 2020, doi: 10.1002/mp.14069.

[10] A. Maldera, P. De Marco, P. E. Colombo, D. Origgi, and A. Torresin, 'Digital breast tomosynthesis: Dose and image quality assessment', *Phys. Medica*, vol. 33, pp. 56–67, 2017, doi: 10.1016/j.ejmp.2016.12.004.

[11] K. H. Thung and P. Raveendran, 'A survey of image quality measures', 2009, doi: 10.1109/TECHPOS.2009.5412098.

[12] D. M. Chandler, 'Seven Challenges in Image Quality Assessment: Past, Present, and Future Research', *ISRN Signal Process.*, vol. 2013, pp. 1–53, Feb. 2013, doi: 10.1155/2013/905685.

[13] M. J. M. Vasconcelos and L. Rosado, 'No-reference blur assessment of dermatological images acquired via mobile devices', *Lect. Notes Comput. Sci. (including Subser. Lect. Notes Artif. Intell. Lect. Notes Bioinformatics)*, vol. 8509 LNCS, pp. 350–357, 2014, doi: 10.1007/978-3-319-07998-1_40.

[14] B. T. Koik and H. Ibrahim, 'A literature survey on blur detection algorithms for digital imaging', in *Proceedings - 1st International Conference on Artificial Intelligence, Modelling and Simulation, AIMS 2013*, 2013, pp. 272–277, doi: 10.1109/AIMS.2013.50.

[15] R. A. Pagaduan, M. C. R. Aragon, and R. P. Medina, 'iBlurDetect: Image Blur Detection Techniques Assessment and Evaluation Study', in *International Conference on Culture Heritage, Education, Sustainable Tourism, and Innovation Technologies (CESIT2020)*, 2020, pp. 286–291, doi: 10.5220/0010307702860291.

[16] G. T. Shrivakshan and C. Chandrasekar, 'A Comparison of various Edge Detection Techniques used in Image Processing', *Int. J. Comput. Sci. Issues*, vol. 9, no. 5, pp. 269–276, 2012, Accessed: Nov. 16, 2021. [Online]. Available: www.IJCSI.org.

[17] R. Bansal, G. Raj, and T. Choudhury, 'Blur image detection using Laplacian operator and Open-CV', *Proc. 5th Int. Conf. Syst. Model. Adv. Res. Trends, SMART 2016*, pp. 63–67, 2017, doi: 10.1109/SYSMART.2016.7894491.

[18] J. L. Pech-Pacheco, G. Cristöbal, J. Chamorro-Martínez, and J. Fernândez-Valdivia, 'Diatom autofocusing in brightfield microscopy: A comparative study', in *Proceedings - International Conference on Pattern Recognition*, 2000, vol. 15, no. 3, pp. 314–317, doi: 10.1109/icpr.2000.903548.

[19] R. Chauhan, K. K. Ghanshala, and R. C. Joshi, 'Convolutional Neural Network (CNN) for Image Detection and Recognition', in *First International Conference on Secure Cyber Computing and Communication (ICSCCC)*, Jul. 2018, pp. 278–282, doi: 10.1109/ICSCCC.2018.8703316.

[20] R. Girshick and J. Malik, 'Training deformable part models with decorrelated features', *Proc. IEEE Int. Conf. Comput. Vis.*, pp. 3016–3023, 2013, doi: 10.1109/ICCV.2013.375.

[21] R. Girshick, J. Donahue, T. Darrell, and J. Malik, 'Region-Based Convolutional Networks for Accurate Object Detection and Segmentation', *IEEE Trans. Pattern Anal. Mach. Intell.*, vol. 38, no. 1, pp. 142–158, Jan. 2016, doi: 10.1109/TPAMI.2015.2437384.

[22] E. Shelhamer, J. Long, and T. Darrell, 'Fully Convolutional Networks for Semantic Segmentation', *IEEE Trans. Pattern Anal. Mach. Intell.*, vol. 39, no. 4, pp. 640–651, Nov. 2014, doi: 10.1109/TPAMI.2016.2572683.

[23] D. Eigen, C. Puhrsch, and R. Fergus, 'Depth Map Prediction from a Single Image using a Multi-Scale Deep Network', *Adv. Neural Inf. Process. Syst.*, vol. 3, no. January, pp. 2366–2374, Jun. 2014, Accessed: Nov. 16, 2021. [Online]. Available: https://arxiv.org/abs/1406.2283v1.

[24] G. Li and Y. Yu, 'Visual saliency detection based on multiscale deep CNN features', *IEEE Trans. Image Process.*, vol. 25, no. 11, pp. 5012–5024, 2016, doi: 10.1109/TIP.2016.2602079.

[25] G. Dong, Z. Zhen, Q. Shi, A. Van Den Hengel, C. Shen, and Y. Zhang, 'Learning deep gradient descent optimization for image deconvolution', *IEEE Trans. NEURAL NETWORKS Learn. Syst.*, vol. 31, no. 12, pp. 5468–5482, 2020.

[26] L. Xu, J. S. Ren, C. Liu, and J. Jia, 'Deep convolutional neural network for image deconvolution', in *Advances in Neural Information Processing Systems*, 2014, vol. 2, no. January, pp. 1790–1798, [Online]. Available: http://www.lxu.me/projects/dcnn/.

[27] N. Zeng, H. Zhang, Y. Li, J. Liang, and A. M. Dobaie, 'Denoising and deblurring gold immunochromatographic strip images via gradient projection algorithms', *Neurocomputing*, vol. 247, pp. 165–172, Jul. 2017, doi: 10.1016/J.NEUCOM.2017.03.056.

[28] N. Zeng, H. Zhang, B. Song, W. Liu, Y. Li, and A. M. Dobaie, 'Facial expression recognition via learning deep sparse autoencoders', *Neurocomputing*, vol. 273, pp. 643–649, Jan. 2018, doi: 10.1016/J.NEUCOM.2017.08.043.

[29] N. Zeng, Z. Wang, H. Zhang, W. Liu, and F. E. Alsaadi, 'Deep Belief Networks for Quantitative Analysis of a Gold Immunochromatographic Strip', *Cogn. Comput. 2016 84*, vol. 8, no. 4, pp. 684–692, Apr. 2016, doi: 10.1007/S12559-016-9404-X.

[30] R. Huang, W. Feng, M. Fan, L. Wan, and J. Sun, 'Multiscale blur detection by learning discriminative deep features', *Neurocomputing*, vol. 285, pp. 154–166, 2018, doi: 10.1016/j.neucom.2018.01.041.

[31] A. Krizhevsky, I. Sutskever, and G. E. Hinton, 'ImageNet classification with deep convolutional neural networks', *Commun. ACM*, vol. 60, no. 6, pp. 84–90, 2017, doi: 10.1145/3065386.

[32] M. Buda *et al.*, 'Detection of masses and architectural distortions in digital breast tomosynthesis: A publicly available dataset of 5,060 patients and a deep learning baseline', *arXiv*, pp. 1–14, 2020.

[33] K. He, X. Zhang, S. Ren, and J. Sun, 'Deep residual learning for image recognition', in *Proceedings of the IEEE Computer Society Conference on Computer Vision and Pattern Recognition*, 2016, vol. 2016-Decem, pp. 770–778, doi: 10.1109/CVPR.2016.90.

[34] K. Simonyan and A. Zisserman, 'Very deep convolutional networks for large-scale image recognition', Sep. 2015, Accessed: Jan. 11, 2022. [Online]. Available: https://arxiv.org/abs/1409.1556v6.

[35] A. Kumar Dash, 'VGG16 Architecture', *Neurohive*, 2018. https://iq.opengenus.org/vgg16/ (accessed Jan. 11, 2022).

[36] C. Szegedy, V. Vanhoucke, S. Ioffe, J. Shlens, and Z. Wojna, 'Rethinking the Inception Architecture for Computer Vision', in *Proceedings of the IEEE Computer Society Conference on Computer Vision and Pattern Recognition*, 2016, vol. 2016-Decem, pp. 2818–2826, doi: 10.1109/CVPR.2016.308.

[37] V. N. Vapnik, 'An overview of statistical learning theory', *IEEE Transactions on Neural Networks*, vol. 10, no. 5. pp. 988–999, 1999, doi: 10.1109/72.788640.